THERMAL ASPECTS OF THE SCUFFING MECHANISM IN ROLLING CONTACTS

Bujoreanu Carmen[1], Chicet Daniela[2]

[1]*Technical University "Gheorghe Asachi" Iaşi ,Mechanical Engineering Faculty, carmen.bujoreanu@gmail.com*
[2]*Technical University "Gheorghe Asachi" Iaşi, Materials Science and Engineering Faculty, daniela_chicet@yahoo.com*

Abstract: *A remarkable feature in the study of scuffing is that confusions and controversies have occupied this research area for many years. Occurrence of scuffing is attributed to different sources. Until now, the most important researches don't establish a unit criterion to be use as safe criteria against scuffing failure. Under particular combinations including contact pressure, lubrication, speed and friction, a critical temperature is reached in the vicinity of the contact. At this temperature, the breakdown film with local welding or adhesion of the contacting surfaces can appear. The paper develops a temperature distribution model for rolling contacts related to the bearings scuffing risk. The observation of the scuffed contact is conducted. Samples from the scuffed region of the inner race are examined by scanning electron microscopy and elemental chemical analysis of EDS type is made. The scuffing phenomenon is discussed after examining and analyzing these photographs.*

Keywords: *temperature, scuffing, rolling contact, metallographic analysis*

1. Introduction

Occurrence of scuffing is attributed to different sources such as instability of hydrodynamic films, desorption of active chemical species [1], destruction of surface films [2], material plastic flow, or accumulation of subsurface damages. The proposed criteria for scuffing show a great variety, including the critical surface temperature [3], maximum PV or PVT values, friction power intensity, subsurface stress, plasticity index, or a combination of temperature, stress and material property.

We can remark the complexity of the scuffing failure phenomena. Until now, the most important researches don't establish a consensus which can be used as safe criteria against scuffing failure.

Investigators who try to understand the mechanisms of scuffing and develop models frequently include temperature as a variable [4]. Attempts have been made to define a critical temperature at which a lubricating film breaks down, leading to a significant rise in friction force. The process that leads to scuffing degrades the hydrodynamic characteristics of the oil film and also undermines the chemically-reactive surface films. Consequently, the knowledge of the local surface temperature becomes important in scuffing evaluation.

The paper presents a temperature distribution model for rolling contacts related to the bearings scuffing risk. Samples from the scuffed region of the inner race were examined by scanning electron microscopy and elemental chemical analysis of EDS type was made. The scuffing phenomenon is discussed after examining and analyzing these photographs.

2. Temperature Distribution Approach

The total contact temperature on the ball race contact ellipse is a sum of both the bulk and flash temperatures. The bulk temperature can be easily measured, but the flash temperature must be calculated [5].

The following assumptions are made:

1.The calculation of flash temperature is based on the theory of a moving heat source over a semi-infinite solid, formulated by Jaeger.

2.The Peclet's number is greater than 10 for the ball races contacts [2], consequently the heat flow in the direction perpendicular to the movement may be neglected.

3. The scuffing failure event is characterized by important sliding speed on the ball bearing contact ellipse (especially on the inner one) and similar to the rolling speed. The difference between the ball and inner race temperatures is significant. That justifies an unequal heat partition, Λ, on each two contacting surfaces, by:

$$\Lambda = \sqrt{U_{ball} / U_{race}}. \quad (1)$$

4.The temperatures distribution is calculated using an iterative procedure on discretized inner contact ellipse with *(a, b)* axis. P(χ) is a point on this surface contact area.

2.1 Computation

To evaluate flash temperatures, T_f, on rolling direction, we considered:

$$T_{f\,ball} = A \cdot \int_{y_0}^{y_{i+1}} f(T,q) \cdot \frac{d\chi}{\sqrt{y_{i+1} - \chi}}. \quad (2)$$

$$T_{f\,race} = B \cdot \int_{y_0}^{y_{i+1}} g(T,q) \cdot \frac{d\chi}{\sqrt{y_{i+1} - \chi}}. \quad (3)$$

To evaluate surface temperatures, T_c , we add the flash temperature as above computed to the average temperature T_m , measured by an infrared thermometer.

$$T_{cball}(y) = T_{m\,ball} + A \cdot \int_{-b}^{y} f(T,q) \cdot \frac{d\chi}{\sqrt{y - \chi}}. \quad (4)$$

$$T_{crace}(y) = T_{m\,race} + B \cdot \int_{-b}^{y} g(T,q) \cdot \frac{d\chi}{\sqrt{y - \chi}}. \quad (5)$$

where the notations made are:

$$A = \sqrt{\frac{1}{\pi \rho_s c_s u_{ball} k_s}}; \; B = \sqrt{\frac{1}{\pi \rho_s c_s u_{race} k_s}}. \quad (6)$$

$$f(T,q) = \frac{k_f}{h_c} \cdot \left(T_{crace(\chi)} - T_{cball(\chi)}\right) + \Lambda \cdot q_{ball(\chi)}. \quad (7)$$

$$g(T,q) = \frac{k_f}{h_c} \cdot \left(T_{cball(\chi)} - T_{crace(\chi)}\right) + (1 - \Lambda) \cdot q_{race(\chi)} \quad (8)$$

u_{ball} , u_{race} - ball and inner race tangential speed.

k_s, k_f - thermal conductivity of solid (ball and inner race) and lubricant.

h_c film central thickness

$T_{c_{ball}(\chi)}$, $T_{c_{race}(\chi)}$ - ball and race surface temperatures in the point of coordinates $(x_j, y_i - \Delta y)$ on the contact ellipse.

$q_{ball(\chi)}$, $q_{race(\chi)}$ - total heat generated by viscous friction $q_f(\chi)$ and the contact asperities $q_a(\chi)$, when there is no complete separation through lubricant in the point of coordinates $(x_j, y_i - \Delta y)$.

Eqs.(2,3,4,5) reflect the cumulative character of energy dissipated on ellipse contact.

The temperature of every point on ball-race contact takes account of three essential components:

$(k_f / h_c) \cdot \left[T_{c_{race(ball)}} - T_{c_{ball(race)}}\right]$ - the heat generated by the thermal transfer through lubricant, between ball and race;

$q_f(\chi) = \tau(\chi) \cdot V(\chi)$ - the energy dissipated as the result of the viscous friction;

$q_a(\chi) = FA \cdot V(\chi)$ - the energy dissipated as result of direct contact on asperities, when there is no complete separation through lubricant.

There are: $\tau(\chi)$ - the lubricant shear stress; $V(\chi)$ - the ball-race sliding speed; *FA* - the asperities friction force. They are computed as described in [6]

The amount of these components in the temperatures computation is strongly related to the bearing lubrication regime and the tangential and sliding speeds of contact surfaces.

2.2 Experiment

Scuffing tests were performed on 7206 angular contact ball bearing included in an original test, as in Fig. 1.

The test equipment is adapted on four-ball machine from our laboratory. The operating speed on the test rig was moderate (max. 2800 rpm), so the ball-inner ring sliding speed too. As the bearing scuffing risk is deeply correlated to high sliding speed (typical to high-speed ball bearings) we realised these conditions by the cage's braking. It were obtained sliding speeds enough high to initiate scuffing phenomenon for a boundary lubrication regime. The speed transducers quantify the braked cage speed and the braking torque,

implicitly the force between ball and cage. With these two known parameters, the correlation between experimental and theoretical investigations can be settled.

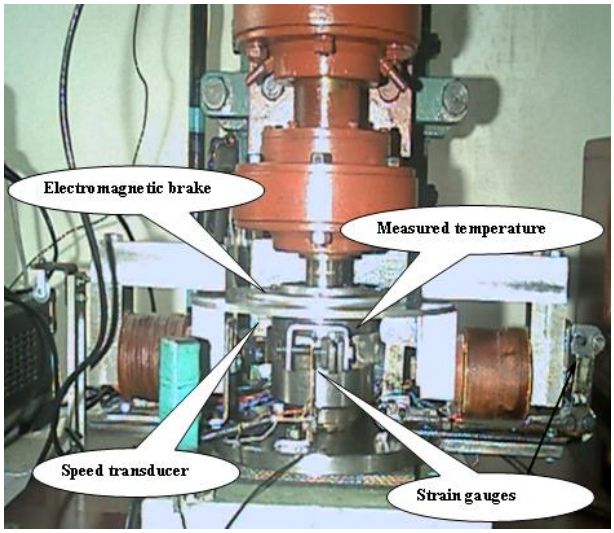

Figure 1: *Scuffing test device*

The test rig also allows measuring the friction torque by means of strain gauges. The sudden increase of the friction force indicates the scuffing occurrence. A Raynger MX4 infrared thermometer has measured average bearing temperature when the scuffing is initiated.

2.3 Critical Scuffing Temperature

The scuffing analysis on bearing's contacts have detached the idea that, any scuffing mechanism considered, there is an energetically unbalance in the rolling contact.

The scuffing failure is the result of a permanent competition between speed and pressure in the contact. We consider an adequate model to estimate the scuffing limits an energetically one.

Energy dissipation quantified by $\mu \cdot p \cdot V^{0.8}$ criterion [6] is corroborated with scuffing temperature.

The temperature distribution model under a particular combination including contact pressure, lubrication, speed and friction estimates the scuffing critical temperature.

For bearing normal operating conditions, with negligible sliding on ball-inner race, the Fig. 2 presents the ball and race surface temperature distributions. They are obtained across the rolling direction on the contact ellipse, according to the computation model above described and using the mineral lubricant ELF 154 NS.

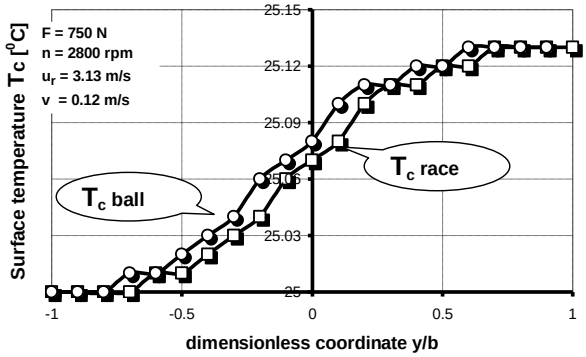

Figure 2: *Surface temperature distribution (T_m = 25 ^{0}C)*

The sliding speeds are very small (v = 0.12 m/s) compared to rolling speed (u_r = 3.13 m/s). This is the reason why the flash temperatures T_f are almost the same on ball and inner race and the surface temperature T_c has no significant rise.

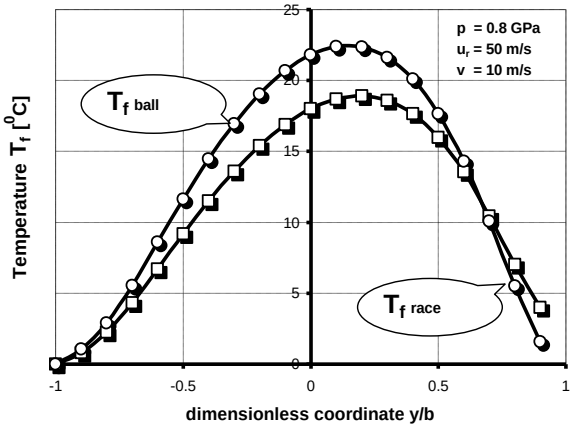

Figure 3: *Flash temperature distribution*

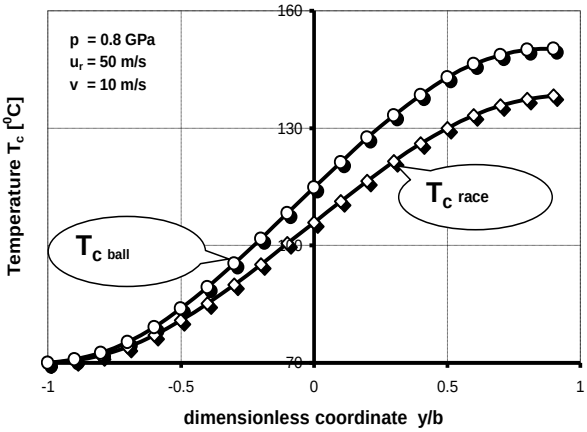

Figure 4: *Surface temperature distribution (T_m = 70 ^{0}C)*

Figures 3 and 4 present the temperature distributions, T_f and T_c, respectively, for another operating conditions, when the rolling and sliding speeds are considerably greater (v = 10 m/s, u_r =

50m/s) than those from the precedent example. It can be noticed the important increase of contact temperatures values. There is the result of the gross sliding measured on the contact.

These high temperatures values involve the scuffing risk for the contact subjected to sliding. Consequently, the contact surface temperatures are presented in Fig. 5 for a slide to roll ratio ξ = 76,5% on the inner race-ball contact ellipse.

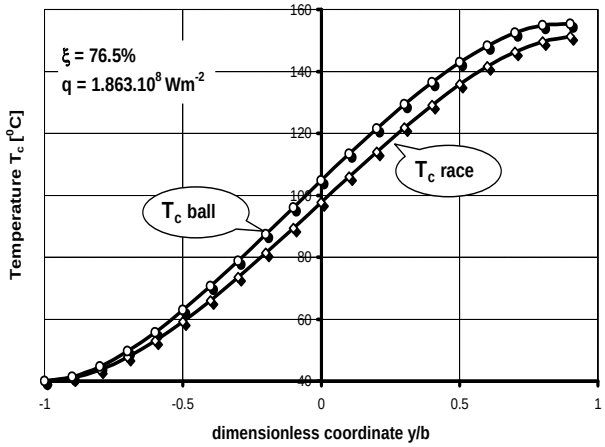

Figure 5: *Surface temperatures with scuffing risk*

It can be remark that the computed temperature with scuffing risk exceeds 150 ^{0}C. These scuffing critical values obtained by the temperature distribution model as above presented are in good agreement with temperature experimental values *(≈160 ^{0}C)* measured with infrared thermometer.

3. Scuffing Metallographic Investigation

Due to the high interest in better understanding of the scuffing failure mechanisms, the attention must be also directed to the material behavior.

We must recognize the fact that the material of the near-surface area is the last one that resist in the series of events that lead to surface scuffing, after the lubrication film breakdown. In order to make some connections between the scuffing phenomenon and the near-surface material behavior, we analyzed the microstructures of the race surface before and after the scuffing occurred.

Figures 6 a, b present the microstructure of studied bearing race surface before the test (Fig.6a) and after the scuffing occurrence (Fig.6b). For this purpose, the areas were metallographically prepared through fine polishing and etching with nital 3%. The surfaces were not grinded in order to obtain the near-surface microstructure (the removed depth should not be bigger than 20-30 microns).

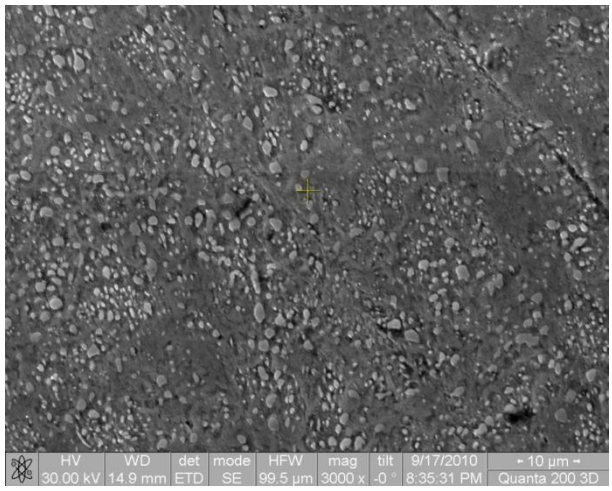

Figure 6a: *Race surface microstructure before the test*

The images were obtained from a scanning electron microscope Quanta 3D type, using the following working conditions: High Vacuum module, ETD detector for secondary electron images and tilt of sample (if required).

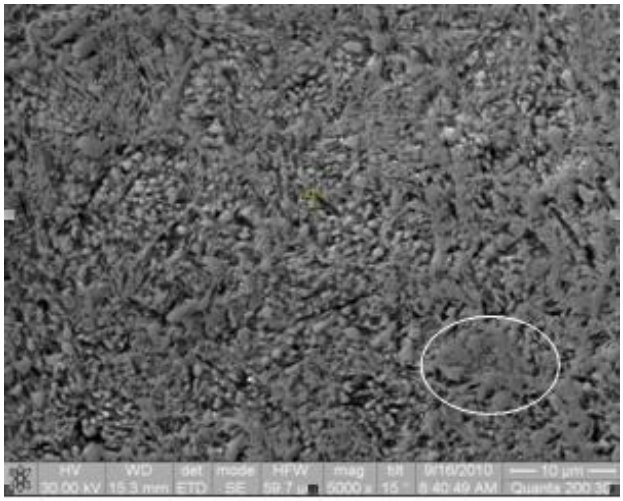

Figure 6b*: Race surface microstructure after the test*

It can be observed in both images that the specific microstructure of this bearing steel (lamellar pearlite with chromium carbides) did not suffer major transformations as a result of scuffing. This observation sustain the critical scuffing temperature (152.2 ^{0}C for the race surface) computed with the temperature distribution model above presented, which is not yet sufficient to produce visible microstructure transformations.

Though, the scuffing phenomenon is accompanied by severe wear tracks, macro plastic flow marks and welds over the frictional area [7,8].

The race near-surface suffers a plastic deformation, with visible consequences as in Fig. 6b. We can see some areas where the microstructure is not that visible - the pearlite lamellas looks almost stuck together with the carbides. They correspond to areas subjected to severe plastic deformation where welds occurred or macro plastic debris delaminated.

In order to ensure that there were no microstructure transformations, we performed an EDS analysis on a carbide (Fig.7a). This is a detail from Fig. 6b, taken from an area where plastic deformation occurred in more visible manner (marked with a red cross). The results presented in Fig. 7b (a higher content of chromium than in other areas) show that the carbides are still there and the structure is the same as before the test, with only slight modifications caused by the plastic deformation phenomenon.

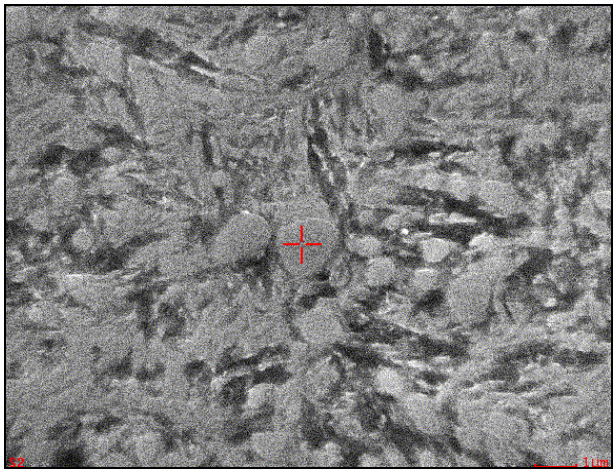

Figure 7a: *The microstructure of an area subjected to EDS analysis*

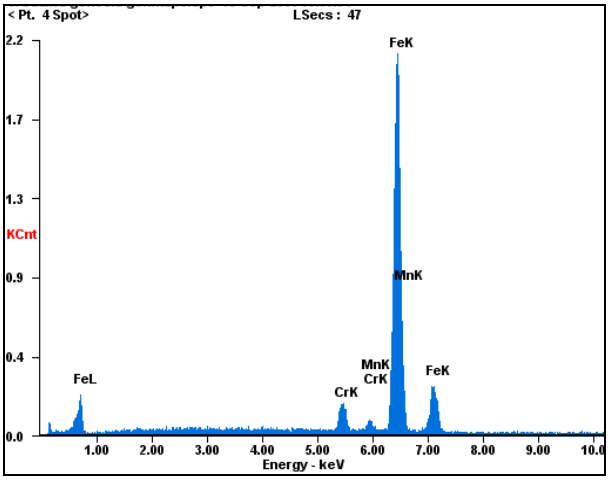

Figure 7b: *EDS analysis of a carbide area (marked on Figure 7a)*

Figures 8,9 present micrographs of some areas were this phenomenon occurred. The images were also obtained using scanning electron microscopy, only that in this case the surfaces were not prepared or modified. Figure 8 highlights the presence of some deep wear tracks at the "edge" of the race surface and also some point-like wear marks caused most likely by the adhesion on the bearing ball of some debris. Figure 9 presents an area with visible macro plastic flow marks on the race surface, caused by severe plastic deformation and delamination.

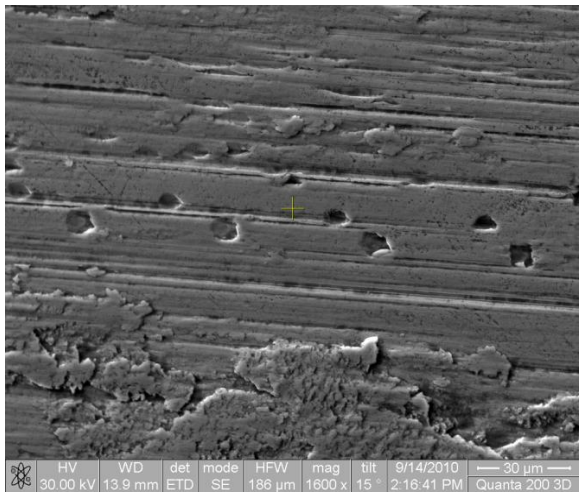

Figure 8: *Race surface wear micrograph – wear tracks and plastic flow marks.*

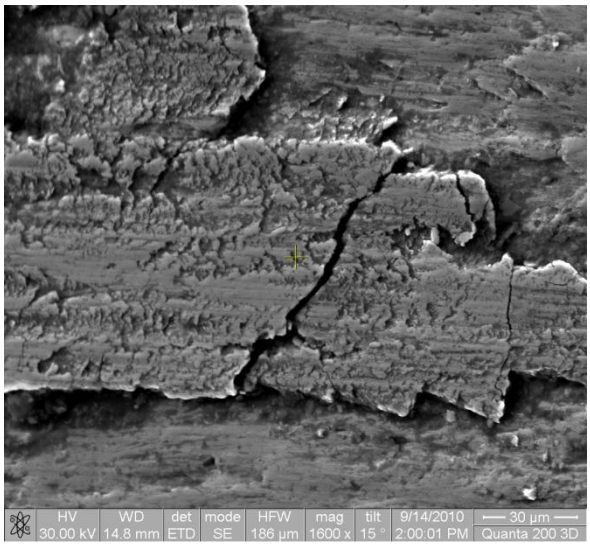

Figure 9: *Race surface wear micrograph – severe macro plastic flow mark*

4. Conclusions

Until now it has not been established a safe criteria against this failure type. The context of any scuffing model is usually limited in applicability.

Our theoretical approach relies on the energetically equilibrium in the bearing rolling contact including the scuffing critical temperature criteria.

The temperature distribution model is a wide covering one from the scuffing point of view. It includes the thermal transfer between ball and races and also the heat generated both by the viscous friction in lubricant film and the boundary friction on the asperity contact.

Sufficient plastic deformation occurs on the contact surface to determine the change of its appearance. Scuffing, lateral displacement or smearing of surface material can occur without a loss of material.

Scuffing tends to be localized, and some portions of the surface can maintain the same structure while others exhibit noticeable damage. This localization makes difficult a quantitative measurement of the scuffing damage degree.

5. References

[1]. Nélias, D., Seabra, J., Flamand, L., Dalmaz, G., Power Loss Prediction in High-Speed Roller Bearings, *Dissipative Processes in Tribology*, D. Dowson et al., 465-478, 1996.

[2]. Zhu, D., Cheng, H. S., An Analysis and Computational Procedure for EHL Film Thickness, Friction and Flash Temperature in Line and Point Contacts, *Trib. Trans.*, no. 32, 364-370, 1989.

[3]. Lee, S. C., Cheng, H. S., Experimental Validation of Critical Temperature-Pressure. Theory of Scuffing., *Trib. Trans.*,vol 38, no. 3, 738-742, 1995.

[4]. Kazuyuki, Yagi., Yukito, Ebisu. ,Joichi, et al., In Situ Observation of Wear Process Before and During Scuffing in Sliding Contact, *Tribology Letters*, 43, 361–368, 2011.

[5]. Shuangbiao Liu, S.Lannou, Q. Wang, L. Keer, Solutions for Temperature Rise in Stationary/Moving Bodies Caused by Surface Heating With Surface Convection, *Trans. of ASME*, 126, 776-785, 2004.

[6]. Bujoreanu, C., Cretu, S., Nelias, D., An Investigation of Scuffing in Angular Contact Ball-Bearings, *Journal of Tribological Balkan Association*, 4/11, 521-529, 2005.

[7]. O.O. Ajayi, J.G. Hersberger, J. Zhang, H. Yoon, G.R. Fenske, Microstructural evolution during scuffing of hardened 4340 steel-implication for scuffing mechanism, *Tribology International*, 38, 277–282, 2005

[8]. Peter J. Blau, Transient Scuffing of Candidate Diesel Engine Materials at Temperatures up to 600^{o}C, *Project Milestone Report*, 1-23, 2009.